

Trastuzumab-Coated Nanoparticles Loaded With Docetaxel for Breast Cancer Therapy

Dose-Response:
An International Journal
July-September 2019:1-12
© The Author(s) 2019
Article reuse guidelines:
sagepub.com/journals-permissions
DOI: 10.1177/1559325819872583
journals.sagepub.com/home/dos



Xueyan Zhang¹, Jiaxin Liu¹, Xiangyu Li¹, Fang Li¹, Robert J. Lee^{1,2}, Fengying Sun¹ , Youxin Li¹, Zongyu Liu¹, and Lesheng Teng¹ 

Abstract

Docetaxel (DTX) is commonly used for breast cancer treatment. Tween 80 used for DTX dissolution in its clinical formulation causes severe hypersensitivity and other adverse reactions. In this study, trastuzumab (Tmab)-coated lipid-polymer hybrid nanoparticles (PLNs) were prepared, composed of poly (D, L-lactide-co-glycolide), PLGA; polyethylenimine (PEI); and lipids. The PLGA/PEI/lipid formed a hydrophobic core, while Tmab was electrostatically adsorbed on the surface of the PLNs as a ligand that targets human epidermal growth factor receptor 2 (HER2)-positive breast cancer cells. The resulting PLNs, electrostatically adsorbed Tmab-bearing PLGA/PEI/lipid nanoparticles (eTmab-PPLNs), had a mean particle size of 217.4 ± 13.36 nm, a ζ potential of 0.056 ± 0.315 mV, and good stability. In vitro, the eTmab-PPLNs showed increased cytotoxicity in HER2-positive BT474 cells but not in HER2-negative MCF7 cells. Studies of the ability of eTmab-PPLNs to target HER2 were performed. The uptake of eTmab-PPLNs was shown to be dependent on HER2 expression level. Therefore, eTmab-PPLNs provide a promising therapeutic for the treatment of breast cancer.

Keywords

trastuzumab, docetaxel, nanoparticle, targeted delivery, electrostatic adsorption

Introduction

Breast cancer is the second most common malignancy worldwide and the most common cancer among women.¹⁻⁴ Currently, chemotherapy is the most common treatment.^{5,6} Docetaxel (DTX) is a second-line chemotherapeutic for metastatic breast cancer and works by inhibiting microtubule depolymerization and cell cycle arrest.⁷ The antitumor effect of DTX has been shown to be superior to that of paclitaxel.^{8,9} Docetaxel has poor water solubility and its intravenous injection currently requires the addition of a solubilizer, Tween 80, which brings hypersensitivity and other adverse reactions.¹⁰ Therefore, it is desirable to develop a safer drug delivery system for DTX with reduced side effects.

In recent years, nanomedicines have been extensively explored for cancer treatment and have shown the potential to reduce side effects of chemotherapy drugs.¹¹⁻¹⁶ Among them, lipid-polymer hybrid nanoparticles (PLNs) as nanocarriers for the delivery of anticancer drugs have been studied.¹⁷⁻¹⁹ The PLNs combine the advantages of 2 nanoscale drug carriers, liposomes and polymer nanoparticles.²⁰ As nanocarriers, PLNs can passively target to tumor sites through enhanced permeability and retention effect. However, in order to improve the

targeting of PLNs to special tumor tissues or cells, several substances such as antibodies, antibodies fragments, transferrin, aptamers, lectins, and peptides can be attached to the surface of PLNs.^{21,22} Among them, antibodies are the most promising and have been widely used as a targeted therapy.^{23,24}

Trastuzumab (Tmab, aka Herceptin) is a monoclonal antibody against human epidermal growth factor receptor 2 (HER2).²⁵⁻²⁷ Clinically, Tmab is mainly used for the treatment of metastatic breast cancer with overexpression of HER2.²⁸ Human epidermal growth factor receptor 2 is an important marker of breast cancer, which is overexpressed in 25% to 30% of invasive breast cancers.²⁹⁻³¹

¹ School of Life Sciences, Jilin University, Changchun, Jilin, China

² College of Pharmacy, The Ohio State University, Columbus, OH, USA

Received 8 May 2019; received revised 28 July 2019; accepted 2 August 2019

Corresponding Authors:

Youxin Li and Lesheng Teng, School of Life Sciences, Jilin University, Changchun, Jilin 130012, China.

Emails: liyouxin@jlu.edu.cn; tenglesheng@jlu.edu.cn



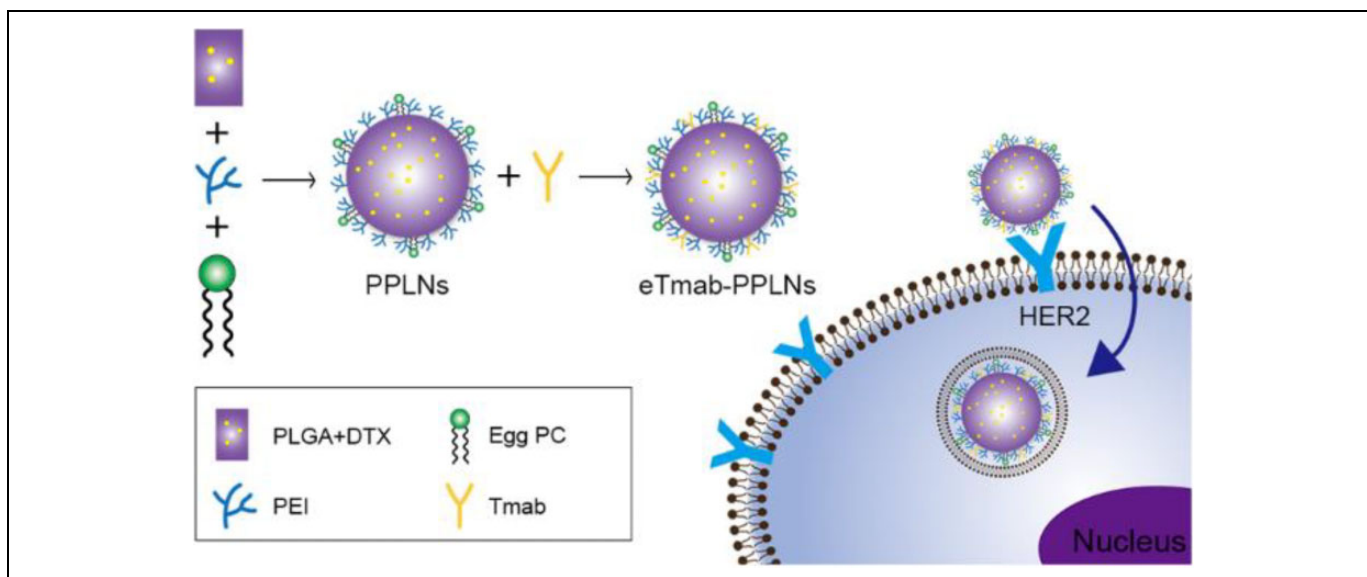


Figure 1. Schematic illustration of the eTmab-PPLNs and their cellular uptake. eTmab-PPLNs indicate electrostatically conjugated trastuzumab-bearing poly (D, L-lactide-co-glycolide)/polyethylenimine/lipid nanoparticles.

Here, we first prepared DTX-loaded PLNs composed of poly (D, L-lactide-co-glycolide), PLGA; lipid; and polyethylenimine (PEI); wherein PEI is a cationic polymer.^{32,33} Electrostatic adsorption was used to connect the PLNs to Tmab to enable targeting of the nanoparticle carrier as shown in Figure 1.³⁴ The figure describes the composition of the electrostatically adsorbed Tmab-bearing PLGA/PEI/lipid nanoparticles (eTmab-PPLNs) and the mechanism of HER2-mediated delivery of eTmab-PPLNs into cells. Physical and chemical properties of the nanocarriers were studied. Then eTmab-PPLNs were evaluated in HER2-positive BT474 cells and HER2-negative MCF7 cells.³⁵

Materials and Methods

Materials

Docetaxel was provided by Yew Pharmaceutical Co, Ltd (Jiangsu, China). Polyethylenimine (branched, molecular weight [Mw] 25 kDa) and poly (vinyl alcohol), PVA (87%-89% hydrolyzed, Mw 13 000-23 000 Da), were purchased from Sigma-Aldrich (St Louis, Missouri). Poly (D, L-lactide-co-glycolide), acid-terminated, lactide/glycolide ratio 50/50, Mw 24 000-38 000 Da, was supplied by Sigma-Aldrich (St Louis). Trastuzumab (Mw 145.5 kDa) was supplied by LuyePharma (Yantai, China). Dichloromethane (DCM) was purchased from Beijing Chemical Works (Beijing, China). Dimethyl sulfoxide (DMSO) was provided by Beijing Solarbio Science & Technology Co, Ltd (Beijing, China); MCF7 and BT474 breast cancer cells were provided by the American Type Culture Collection (Manassas, Virginia).

Nanoparticles Preparation

Preparation of PLGA/PEI/lipid nanoparticles. The emulsion solvent evaporation/diffusion method was used to prepare PLGA/PEI/lipid nanoparticles (PPLNs).^{36,37} Briefly, PEI, PLGA, and egg phosphatidylcholine (PC) were dissolved in 1 mL of DCM. Then, 3 mg of DTX was added and ultrasonically dispersed to obtain the organic phase. Thereafter, the organic phase was slowly transferred into 2 mL 2% (wt/vol) PVA and emulsified using sonication for 3 minutes at 300 W in an icebath. Then, 20 mL deionized water was poured into the obtained emulsion. The emulsion was stirred at room temperature for 4 hours on a magnetic stirrer to evaporate the organic solvent. The resulting emulsion was centrifuged (18 000 rpm, 15 minutes, 4°C; Allegra 64R; Beckman Coulter Corp, Brea, California) to pellet PPLNs. Then, the PPLNs were washed with deionized water to remove unencapsulated DTX and excess PEI. The final PPLNs were resuspended in approximately 1 mL deionized water and lyophilized. Finally, the lyophilized PPLNs were stored at 4°C for further use. The PPLNs loaded with rhodamine B were prepared using the same method except for replacing DTX with rhodamine B. In addition, blank PPLNs were prepared by the same method, except DTX was not added.

Preparation of electrostatically conjugated trastuzumab-bearing PPLNs. The eTmab-PPLNs were prepared as described previously.³⁸ Briefly, lyophilized PPLNs and Tmab were dispersed in phosphate buffer solutions (PBS, pH 6.0) at different incubation ratios (4:1, 2:1, 1:1, 1:2, 1:4), and mixed well. The mixed solution was incubated with shaking at 25°C for 1 hour. The product was dialyzed in deionized water, and eTmab-PPLNs were collected and freeze-dried for further use.

Characterization of Nanoparticles

Particle size analysis and ζ potential measurement. Particle size, polydispersity index (PDI), ζ potential of PPLNs, and eTmab-PPLNs were examined by dynamic light scattering (DLS) at 25°C on a Zetasizer Nano ZS90 from Malvern (Worcestershire, United Kingdom). Particle size referred to the diameter of the particle. The PPLNs and eTmab-PPLNs were resuspended in deionized water to 1 mg/mL, and then ultrasonically dispersed for 30 seconds before measurement. Each sample was measured 3 times.

Drug loading and encapsulation efficiency. The drug loading (DL) and encapsulation efficiency (EE) were obtained by directly measuring the amount of DTX in various PPLNs or eTmab-PPLNs using high-performance liquid chromatography (HPLC). The analysis was performed at 230 nm using an Extend-C18 column (4.6 mm \times 250 mm). In short, 2 mg of lyophilized nanoparticles were accurately weighed and redissolved in 2 mL of acetonitrile. After sonicating for 5 minutes, 2 mL of ultrapure water was added and mixed for HPLC analysis. According to the full-wavelength scan, the maximum absorption wavelength of DTX was 230 nm. The total amount of DTX in the PPLNs or eTmab-PPLNs was determined from the peak area, which was correlated with a standard curve. All samples were analyzed 3 times. The EE and DL of the nanoparticles were calculated by the following Equations (1) and (2):

$$EE = \frac{\text{The quality of the encapsulated DTX in nanoparticles}}{\text{Total quality of DTX actually used}} \times 100\% \quad (1)$$

$$DL = \frac{\text{The quality of DTX in nanoparticles}}{\text{The quality of nanoparticles}} \times 100\% \quad (2)$$

The amount of Tmab that was electrostatically adsorbed to the surface of PPLNs was measured indirectly. The supernatant of each centrifugal step was collected for quantitative analysis. After dilution or concentration, the amount of Tmab was analyzed using the bicinchoninic acid (BCA) method. In short, 20 μ L of a series concentration of Tmab and the supernatant were added to the 96-well plate. After that, 200 μ L of BCA working solution was added. Then they were incubated at 37°C for 30 minutes before optical density was measured at 562 nm using a microplate reader. The binding efficiency (BE) of Tmab was calculated using the following Equation (3):

$$BE = \frac{\text{Total amount of Tmab added} - \text{Amount of free Tmab in supernatant}}{\text{Total amount of Tmab added}} \times 100\% \quad (3)$$

Morphological representation. The morphology and size of PPLNs and eTmab-PPLNs were investigated by transmission electron microscopy (TEM, H-800, Hitachi, Japan). Briefly, the PPLNs and eTmab-PPLNs were suspended in deionized water to 1 mg/mL and kept on copper grid and left to air dry overnight. The PPLNs and eTmab-PPLNs were visualized at accelerating voltage of 200 kV with 100 000 \times magnification.

Stability of eTmab-PPLNs

In order to study the stability of eTmab-PPLNs under physiological (37°C) and storage conditions (4°C), eTmab-PPLNs were diluted at a concentration of 1.0 mg/mL with 2 media, PBS (0.02 mol/L, pH 7.4) and PBS with 10% fetal bovine serum (FBS, vol/vol) added. The eTmab-PPLNs in different media were incubated at 37°C and 4°C. Samples were taken at specified time points to acquire the mean particle size and PDI of eTmab-PPLNs.

Hemolysis Test

Since the designed mode of administration was intravenous administration, a hemolysis test was conducted as described previously.³⁹ Briefly, fresh blood was collected from the orbit of rats. The samples were centrifuged at 1400g for 15 minutes at 4°C to get the red blood cells (RBCs) after dilution with physiological saline (0.9% NaCl). Then, RBCs were washed with saline 3 times and diluted at a concentration of 2% (vol/vol). Different concentrations of the PPLNs and eTmab-PPLNs suspension were added to the RBCs suspension and gently vortexed. All the samples were incubated in a water bath for 3 hours at 37°C; 1% Triton X-100 and saline-treated RBCs were used as a positive and negative control, respectively.

In Vitro DTX Release Study

Drug release from DTX-loaded PPLNs and eTmab-PPLNs was performed by dialysis. The nanoparticles were suspended in 2 mL of release fluid consisting of PBS (0.01 mol/L, pH 7.4) containing 0.5% Tween 80 (vol/vol) and were sealed in a dialysis bags (with a molecular weight cutoff of 7 kDa). Afterward, the dialysis bags were immersed in 30 mL of release fluid and incubated in a shaker (120 rpm) at 37°C. Then, 2 mL of the solution was taken at the specified time point (1, 2, 4, 8, 24, and 48 hours), and 2 mL of freshly prepared release medium was added. Concentrations of released DTX were measured using HPLC method.

In Vitro Cell-Line Studies

Cell cultures. The HER2-positive BT474 cells and HER2-negative MCF7 cells were grown in Dulbecco modified Eagle medium and Roswell Park Memorial Institute-1640 medium, respectively, which was supplemented with 10% FBS, 100 IU/mL of penicillin, and 100 mg/mL of streptomycin (37°C, CO₂).

Cytotoxicity assay. The MCF7 and BT474 cells in the logarithmic growth phase were seeded in the 96-well plates (1.0 \times 10⁴ cells/well) and cultured overnight in a CO₂ incubator. On the next day, the original medium was replaced with fresh medium containing a different concentration of DTX, Tmab, PPLNs, eTmab-PPLNs, and pTmab-PPLNs (PPLNs were physically mixed with Tmab). Then, 48 hours later, 20 μ L 3-(4,5-Dimethylthiazol-2-yl)-2,5-diphenyltetrazolium bromide (MTT) (5 mg/mL) was added and incubated for an additional

Table 1. Effect of PLGA-to-egg PC Ratio on Characteristics of PPLNs.^a

PLGA:Egg PC (wt/wt)	Size, nm	PDI	ζ potential, mV	EE, %
8:0	191.0 ± 1.901	0.103 ± 0.039	-5.14 ± 0.310	34.02 ± 0.955
7:1	181.7 ± 3.554	0.147 ± 0.041	-6.09 ± 0.906	39.88 ± 6.756
6:2	171.7 ± 1.007	0.114 ± 0.041	-6.55 ± 0.688	17.23 ± 0.110
5:3	157.3 ± 1.150	0.081 ± 0.056	-9.89 ± 1.22	10.65 ± 0.630
4:4	152.4 ± 4.678	0.156 ± 0.046	-10.2 ± 0.273	13.85 ± 0.296

Abbreviations: EE, encapsulation efficiency; egg PC, egg phosphatidylcholine; PDI, polydispersity index; PLGA, poly (D, L-lactide-co-glycolide); PPLNs, PLGA/polyethylenimine /lipid nanoparticles; SD, standard deviation.

^aData are expressed as mean ± SD (n = 3).

4 hours in a CO₂ incubator. Finally, the supernatant was removed and 150 μL of DMSO was added to dissolve the formazan crystals, which was converted from MTT in live cells. After further incubation for 10 minutes, the absorbance was measured at 490 nm wavelength using plate reader. Cell viability of each group was expressed as a percentage to that of untreated control cells.⁴⁰

Confocal microscopy. The cellular uptake of PPLNs and eTmab-PPLNs was studied by confocal laser scanning microscopy (CLSM). The eTmab-PPLNs used in the cell uptake experiments were double fluorescently labeled nanoparticles, in which rhodamine B-labeled PPLNs and fluorescein isothiocyanate (FITC)-labeled Tmab were incorporated. The preparation of rhodamine B-loaded PPLNs was described in the preparation of PLGA/PEI/lipid nanoparticles. The FITC-labeled Tmab was prepared as follows: The FITC solution dissolved in DMSO at 1 mg/mL was slowly added dropwise to Tmab dissolved in pH 9.0 carbonate buffer solution (Tmab:FITC = 1:7), and the solution was incubated in the dark at 4°C for 8 hours. The product was dialyzed in PBS (pH 7.4) to remove free FITC.

The MCF7 and BT474 cells were seeded into 12-well plate at a density of 2×10^5 cells per well and cultured overnight. The original medium was replaced, and double fluorescently labeled eTmab-PPLNs with the fresh culture medium diluted (DTX concentration of 2 μmol/L) were added. After 2 hours, the original medium was removed, and the cells were washed with the cold PBS and fixed with 4% paraformaldehyde (PFA) for 15 minutes. The nuclei were stained with 4',6-diamidino-2-phenylindole (DAPI) for 4 minutes. In order to investigate the Tmab targeting of eTmab-PPLNs, free unlabeled Tmab (200 μmol/L) was added to the medium 1 hour before drug administration for competitive HER2 blockade. The nanoparticles were observed under CLSM on an LSM710 from Carl Zeiss Meditec (Jena, Germany).

Flow cytometry. Similarly, the cellular uptake of PPLNs and eTmab-PPLNs was also studied by flow cytometry. Briefly, BT474 and MCF7 cells were seeded into 24-well plates (2×10^5 cells) and incubated overnight. The culture medium was replaced, and double fluorescently labeled eTmab-PPLNs with the fresh culture medium diluted (DTX concentration of 2 μmol/L) were added. After 2 hours, the cells washed with

Table 2. Effect of PEI Content on Characteristics of PPLNs.^a

Quality of PEI in O phase, mg	Size, nm	PDI	ζ potential, mV
0	202.9 ± 2.325	0.114 ± 0.014	-3.39 ± 0.595
1	221.8 ± 2.194	0.067 ± 0.010	9.05 ± 0.83
2	208.8 ± 5.260	0.129 ± 0.059	15.4 ± 2.51
4	205.9 ± 2.434	0.085 ± 0.017	21.3 ± 1.83
6	196.2 ± 1.701	0.162 ± 0.061	22.0 ± 1.27

Abbreviations: PDI, polydispersity index; PEI, polyethylenimine; PLGA, poly (D, L-lactide-co-glycolide); PPLNs, PLGA/PEI/lipid nanoparticles; SD, standard deviation.

^aPLGA-to-egg PC ratio of 7:1 was used to fabricate the PPLNs and data are expressed as mean ± SD (n = 3).

PBS (0.01 mol/L, pH 7.4) for 3 times, harvested using trypsin, and resuspended in PFA for flow cytometry (Beckman Coulter Corp) analysis. As with the laser confocal microscopy study, unlabeled Tmab (200 μmol/L) was added to the medium 1 hour before drug administration for receptor blockade.

Statistical Analysis

The data were expressed as the mean ± SD. The statistical significance was performed by analysis of variance. $P < .05$ was considered a significant difference.

Results

Preparation of Nanoparticles

In order to obtain the nanoparticles that had the suitable particle size, PDI, and ζ potential, several factors including the ratio of PLGA and egg PC and the amount of PEI were investigated. The results are shown in Tables 1 and 2. In Table 1, with the increase of egg PC, the particle size of PPLNs decreased from 191.0 to 152.4 nm, and EE% increased from 34.0% to 39.88% and then decreased to 13.85%. At different ratios of PLGA and egg PC, PDIs were all less than 0.2, indicated that the dispersion of PPLNs was good. Therefore, considering the compromise of particle size and EE, we chose the ratio of PLGA and egg PC (wt:wt) of 7:1 for all subsequent experiments. In Table 2, the ζ potential of PPLNs gradually increased with the increase of the PEI ratio in the oil phase, but when the amount of PEI was increased from 4 to 6 mg, the ζ potential increase

Table 3. Effect of Antibody Content on Characteristics of eTmab-PPLNs.^{a,b}

PPLNs-to-Tmab (wt/wt)	PPLNs			eTmab-PPLNs			
	Size, nm	PDI	ζ potential, mV	Size, nm	PDI	ζ potential, mV	BE, %
1:4				217.4 ± 13.36	0.202 ± 0.029	3.010 ± 0.150	35.09 ± 2.60
1:2				207.9 ± 9.396	0.125 ± 0.021	1.800 ± 0.070	30.72 ± 1.63
1:1	179.3 ± 0.707	0.078 ± 0.020	20.8 ± 0.721	199.1 ± 4.026	0.098 ± 0.009	0.895 ± 0.248	51.01 ± 3.85
2:1				192.5 ± 9.843	0.102 ± 0.032	0.553 ± 0.360	39.09 ± 3.26
4:1				192.6 ± 3.786	0.095 ± 0.034	0.705 ± 0.261	45.68 ± 1.48

Abbreviations: BE, binding efficiency; eTmab-PPLNs, electrostatically conjugated trastuzumab-bearing PPLNs; PDI, polydispersity index; PLGA, PPLNs, poly (D, L-lactide-co-glycolide)/polyethylenimine/lipid nanoparticles;

^aBE is the percentage of the amount of adsorbed Tmab and the total amount of Tmab added.

^bData are represented as mean ± SD (n = 3). SD, standard deviation

Table 4. Characteristics of the Optimized Formulations.^a

Formulation	Size, nm	PDI	ζ Potential, mV	EE, %
PPLNs	193.4 ± 4.204	0.087 ± 0.017	23.6 ± 1.77	35.06 ± 5.703
eTmab-PPLNs	217.4 ± 13.36	0.116 ± 0.057	0.056 ± 0.115	31.27 ± 3.215

Abbreviations: EE, encapsulation efficiency; eTmab-PPLNs, electrostatically conjugated trastuzumab-bearing PPLNs; PDI, polydispersity index; PPLNs, poly (D, L-lactide-co-glycolide)/polyethylenimine/lipid nanoparticles; SD, standard deviation.

^aData are represented as mean ± SD (n = 3).

was not obvious. Therefore, the final determination of the amount of PEI in the oil phase was 4 mg.

The effects of PPLNs-Tmab ratios on ζ potential, particle size, and PDI of eTmab-PPLNs were studied for the preparation of eTmab-PPLNs. As shown in Table 3, when PPLNs-Tmab ratios were low, PPLNs could not effectively bind with Tmab, and there was a large amount of free Tmab in the system. Then, as PPLNs-Tmab ratios increased, BE also increased. When the PPLNs-Tmab ratio was as high as 4:1, BE was high but the amount of reacted Tmab was low when the PPLNs-Tmab ratio was as high as 4:1. When PPLNs-Tmab ratio was 1:1, the BE was the highest.

Characterization of Nanoparticles

According to the appropriate ratios of each material, the PPLNs and eTmab-PPLNs were prepared. The particle size of eTmab-PPLNs was 217.4 ± 13.36 nm as shown in Table 4, which was larger than PPLNs (193.4 ± 4.204 nm). In addition, the ζ potential of eTmab-PPLNs was 0.056 ± 0.315 mV, which was lower than PPLNs (23.6 ± 1.77 mV). In addition, we could see that the EE of eTmab-PPLNs was 31.27% ± 3.215%, which was a little lower than PPLNs (35.06% ± 5.703%). Presumably, Tmab, which was attached to the surface of the PPLNs, prevented the nanoparticles from loading the DTX.

As shown in Figure 2A, eTmab-PPLNs were opalescent and no obvious aggregation in deionized water occurred. The eTmab-PPLNs had a narrow particle size distribution with a mean particle size of 217.4 ± 13.36 nm (Figure 2B). The morphology and size of the prepared PPLNs and eTmab-PPLNs were also detected using TEM. As shown

in Figure 2C and D, PPLNs and eTmab-PPLNs were relatively uniform in size and were spherical.

Stability of eTmab-PPLNs

The eTmab-PPLNs were resuspended in different solutions, and their particle sizes and PDI were measured to determine their stability. As shown in Figure 3A and B, at 4°C, the particle size and PDI of eTmab-PPLNs in FBS-free and 10% FBS pH 7.4 PBS did not change significantly, indicating that eTmab-PPLNs did not aggregate and could be stored for further use. Figure 3C and D showed that, at 37°C, the particle size of eTmab-PPLNs decreased and the PDI increased in pH 7.4 PBS without 10% FBS. This behavior might be due to the partial dissociation of Tmab on the surface of eTmab-PPLNs under physiological pH, which was different from its incubation conditions. Furthermore, the particle size of eTmab-PPLNs first decreased and then increased in pH 7.4 PBS with 10% FBS, which might be due to the partial dissociation of Tmab at the beginning to reduce the particle size of eTmab-PPLNs, and then eTmab-PPLNs adsorbed the serum proteins in the solution to cause the increase of the particle size. During this process, PDI fluctuated with the dissociation of Tmab and the binding of eTmab-PPLNs to the serum protein, and then decreased to near the initial state, indicating that no aggregation occurred.

Hemolysis Test

We performed the hemolysis test to verify the safety of intravenous administration of the nanoparticles. The results of the hemolysis test are shown in Figure 4. In Figure 4, the hemolysis rates of PPLNs and eTmab-PPLNs were less than 2% at a

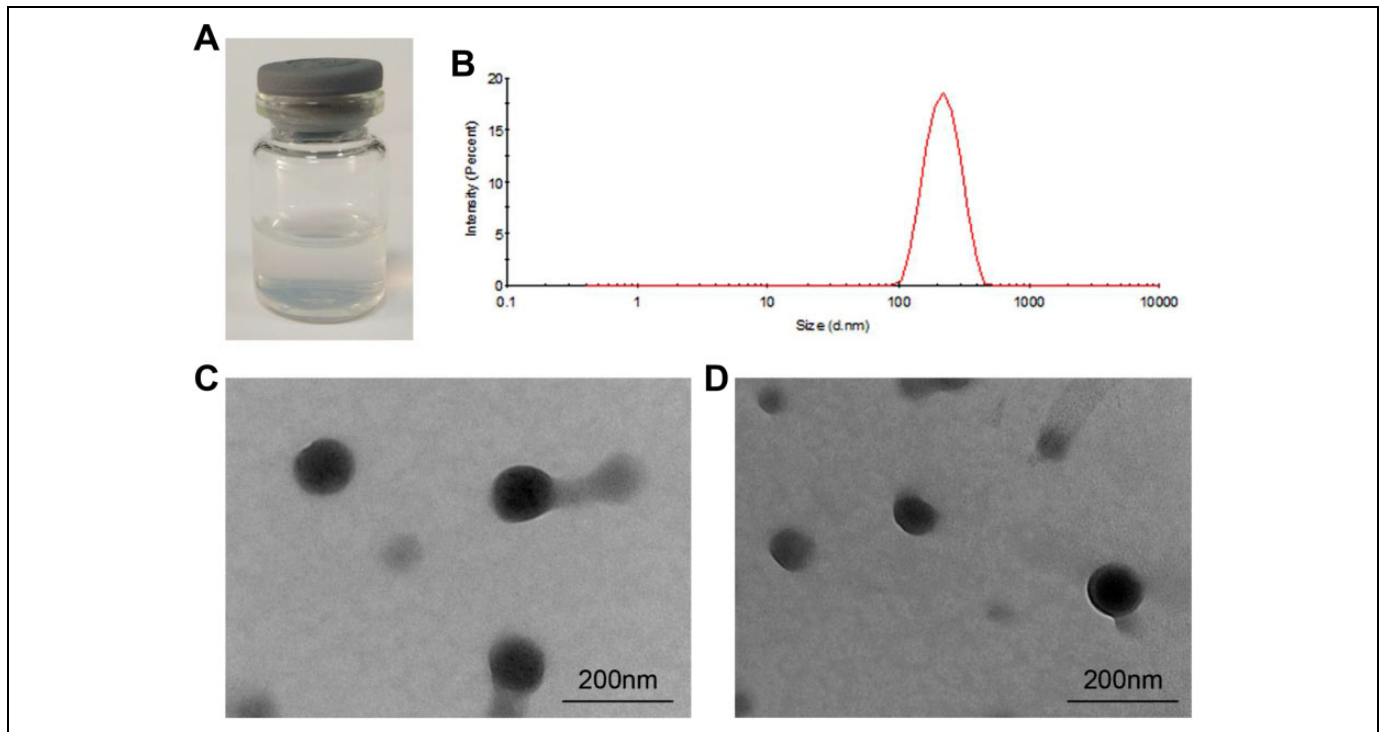


Figure 2. Characteristics of nanoparticles. A, eTmab-PPLNs solution at the concentration of 1 mg/mL. B, Particle size distribution of eTmab-PPLNs. C, TEM image of PPLNs. D, TEM image of eTmab-PPLNs. eTmab-PPLNs indicate electrostatically conjugated trastuzumab-bearing poly(D, L-lactide-co-glycolide)/polyethylenimine/lipid nanoparticles; TEM, transmission electron microscopy.

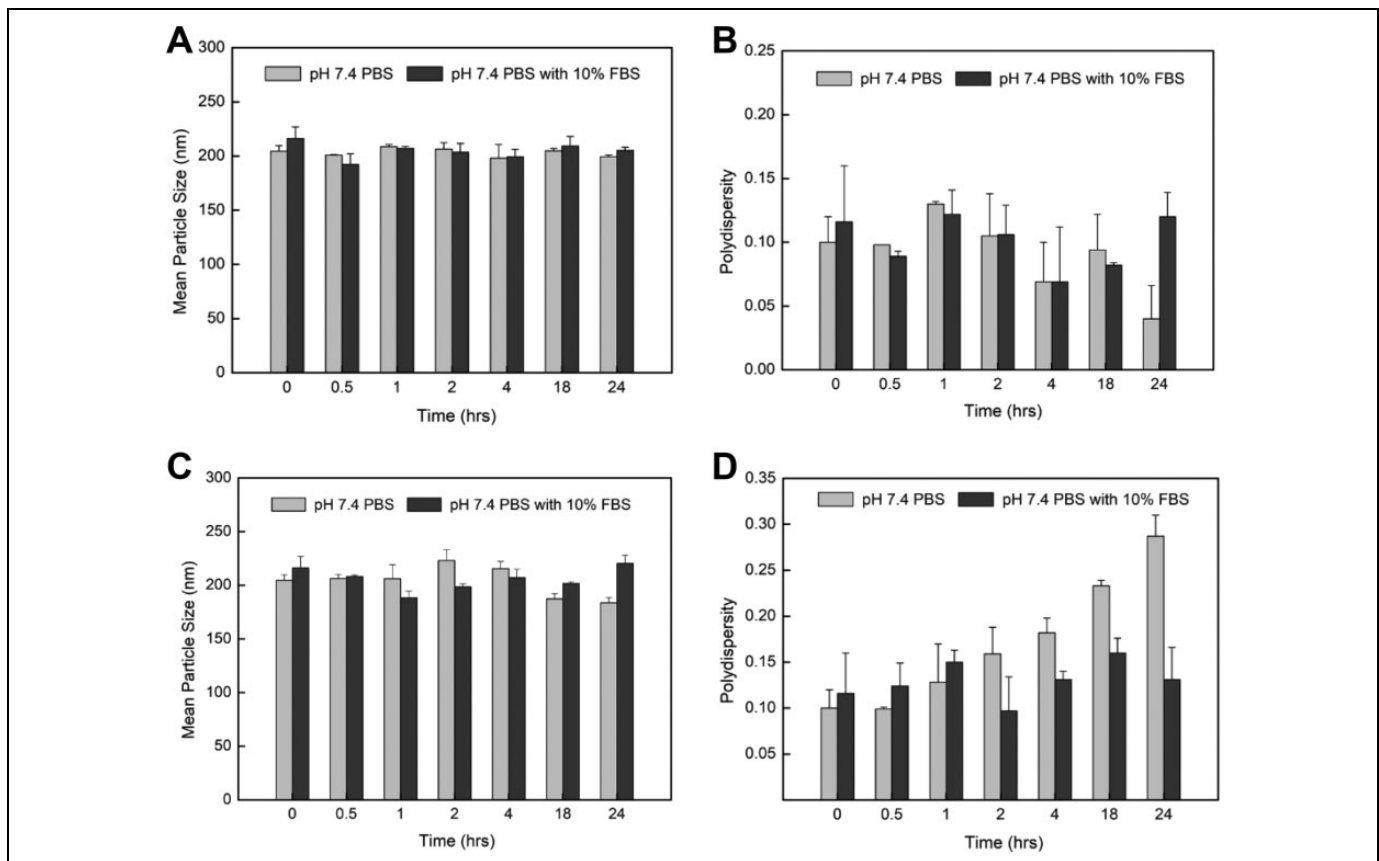


Figure 3. In vitro stability of eTmab-PPLNs. A and B, PDI and size of eTmab-PPLNs in different media at 4°C. C and D, PDI and size of eTmab-PPLNs in different media at 37°C. Values are mean \pm SD (n = 3). eTmab-PPLNs indicate electrostatically conjugated trastuzumab-bearing poly(D, L-lactide-co-glycolide)/polyethylenimine/lipid nanoparticles; PDI, polydispersity index; SD, standard deviation.

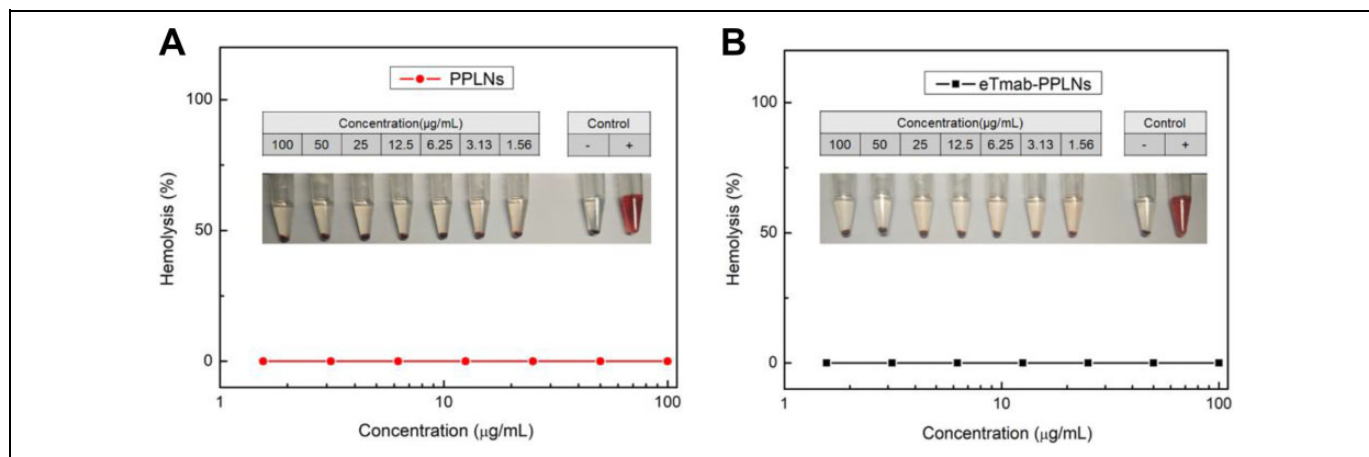


Figure 4. Hemolysis induction by PPLNs and eTmab-PPLNs. A, Hemolysis of PPLNs at different concentrations. B, Hemolysis of eTmab-PPLNs at different concentrations. Values are mean \pm SEM ($n = 6$). eTmab-PPLNs indicate electrostatically conjugated trastuzumab-bearing poly (D, L-lactide-co-glycolide)/polyethylenimine/lipid nanoparticles; SEM, standard error of the mean.

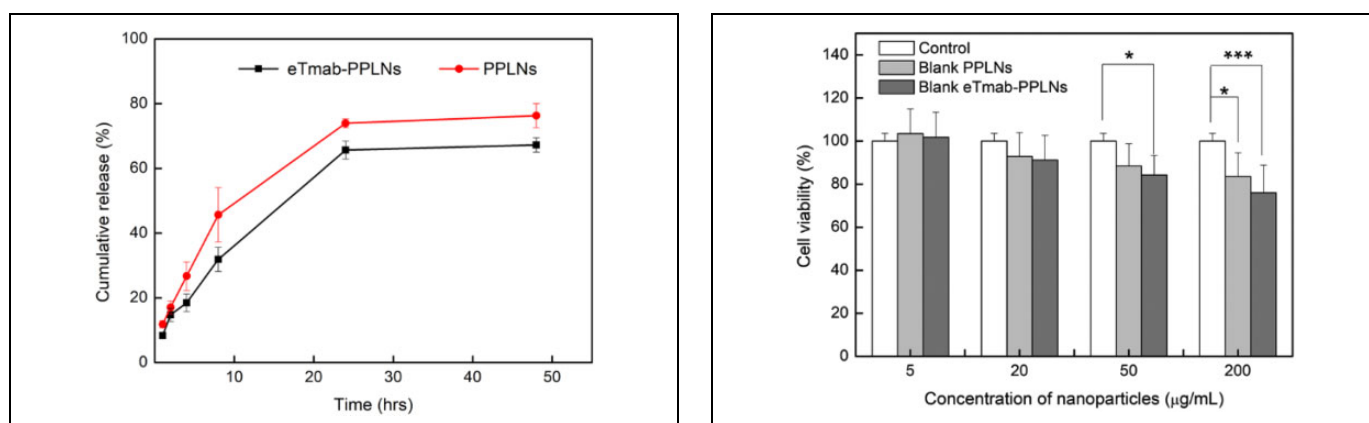


Figure 5. In vitro DTX release from nanoparticles. At 37°C, the release of DTX from PPLNs or eTmab-PPLNs within 48 hours, respectively. Values are mean \pm SD ($n = 3$). DTX indicates docetaxel; eTmab-PPLNs, electrostatically conjugated trastuzumab-bearing poly (D, L-lactide-co-glycolide)/polyethylenimine/lipid nanoparticles; PPLNs, poly (D, L-lactide-co-glycolide)/polyethylenimine/lipid nanoparticles.

Figure 6. Cytotoxicity of blank nanoparticles at different concentrations. BT474 cells were treated with blank PPLNs and blank eTmab-PPLNs at the concentrations of 5, 20, 50, and 200 $\mu\text{g/mL}$ for 48 hour, $n = 6$. eTmab-PPLNs, electrostatically conjugated trastuzumab-bearing poly (D, L-lactide-co-glycolide)/polyethylenimine/lipid nanoparticles; PPLNs, poly (D, L-lactide-co-glycolide)/polyethylenimine/lipid nanoparticles.

series of concentration of DTX (from 1.56 to 100 $\mu\text{g/mL}$). The results indicated that the PPLNs and eTmab-PPLNs had good biocompatibility and were relatively safe for intravenous injection.

In Vitro DTX Release

We observed the release of DTX from PPLNs and eTmab-PPLNs within 48 hours at 37°C. As shown in Figure 5, in the first 10 hours, the nanoparticles showed a burst release. The PPLNs and eTmab-PPLNs released about 45.7% and 31.9% of DTX, respectively. The cause of the burst might be because of the release of DTX distributed on the surface and periphery of the nanoparticles. Then, the 2 nanoparticles had a significant drug release within 10 to 24 hours. Finally, the cumulative in vitro release of PPLNs and eTmab-PPLNs was 76.3% and

67.3%, respectively, indicating that Tmab on the surface of eTmab-PPLNs prevented the release of DTX to some extent.

Cytotoxicity Assay

Firstly, we studied the cytotoxicity of blank nanoparticles. As shown in Figure 6, blank eTmab-PPLNs were more toxic to cells than blank PPLNs at various concentrations, probably due to that Tmab itself had a certain killing effect on cells. We could see that when blank eTmab-PPLNs was 50 $\mu\text{g/mL}$, it showed a certain degree of cytotoxicity ($*P < .05$), and when the concentration of blank nanoparticles was 200 $\mu\text{g/mL}$, blank PPLNs and blank eTmab-PPLNs showed different degrees of cytotoxicity ($P < .05$, $***P < .001$), which was much higher than the use concentration. The HER2-positive BT474 cells and HER2-negative MCF7 cells were selected as subjects to

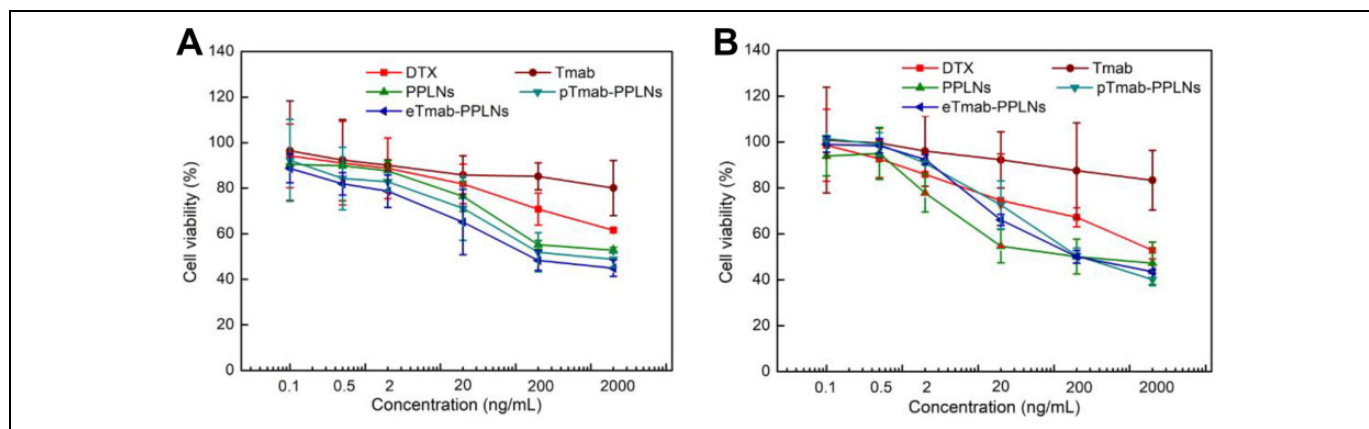


Figure 7. Cytotoxicity of DTX solution, Tmab, PPLNs, pTmab-PPLNs, and eTmab-PPLNs. BT474 (A) and MCF7 (B) cells were treated with DTX solution, Tmab, PPLNs, pTmab-PPLNs, and eTmab-PPLNs at DTX concentrations of 0.1, 0.5, 2, 20, 200 and 2000 ng/mL for 48 hours, $n = 6$. DTX indicates docetaxel; eTmab-PPLNs, electrostatically conjugated trastuzumab-bearing poly (D, L-lactide-co-glycolide)/polyethylenimine/lipid nanoparticles; PPLNs, poly (D, L-lactide-co-glycolide)/polyethylenimine/lipid nanoparticles; Tmab, trastuzumab.

Table 5. IC₅₀ Values of DTX Solution, Tmab, PPLNs, pTmab-PPLNs, and eTmab-PPLNs in BT474 Cells and MCF7 Cells Following 48-Hour Incubation.^a

Cell Line Type	IC ₅₀ Value, $\mu\text{g/mL}$				
	DTX	Tmab	PPLNs	pTmab-PPLNs	eTmab-PPLNs
BT474	10.50 ± 1.25	908.05 ± 70.58	1.89 ± 0.26	0.91 ± 0.15	0.34 ± 0.09
MCF7	2.59 ± 0.85	2519.43 ± 134.09	0.39 ± 0.05	0.38 ± 0.04	0.36 ± 0.02

Abbreviations: DTX, docetaxel; eTmab-PPLNs, electrostatically conjugated trastuzumab-bearing PPLNs; PPLNs, poly (D, L-lactide-co-glycolide)/polyethylenimine/lipid nanoparticles; pTmab-PPLNs, PPLNs physically mixed with Tmab; Tmab, trastuzumab.

^aData are represented as mean \pm SD ($n = 3$).

evaluate the HER2 targeting of eTmab-PPLNs. The overall trends of cytotoxicity of DTX solution, PPLNs, pTmab-PPLNs, and eTmab-PPLNs on BT474 and MCF7 cells were similar as shown in Figure 7A and B. The cytotoxicity increased with increasing concentration of DTX. In contrast, Tmab was less cytotoxicity to both types of cells. Compared with DTX solution, PPLNs, pTmab-PPLNs, and eTmab-PPLNs exhibited significantly greater cytotoxicity for BT474 cells. But for MCF7 cells, this phenomenon was observed at higher concentrations. It was worth noting that for BT474 cells, the eTmab-PPLNs group had lower cell survival than the PPLNs group. However, for MCF7 cells, PPLNs and eTmab-PPLNs did not show differences in cytotoxicity. This result indicated that eTmab-PPLNs had the ability to target the HER2 on tumors. In addition, the cell viability of BT474 cells at various eTmab-PPLNs concentration (44.9%, 48.3%, 65.2%, 78.7%, 81.9%, and 88.7%) after incubation for 48 hours was almost lower than the cell viability of MCF7 cells (43.5%, 45.0%, 66.1%, 92.4%, 98.4%, and 99.2%), suggesting effective targeting of eTmab-PPLNs to HER2. Compared with the eTmab-PPLNs group, BT474 cells treated with pTmab-PPLNs had higher cell survival, indicating that the increased cytotoxicity was due to the endocytosis mediated by HER2, rather than the simple sum of the cytotoxic effects of PPLNs and Tmab.

The half maximal inhibitory concentration (IC₅₀) values of different formulations for different cell lines are shown in Table 5. For BT474 cells, the IC₅₀ value of eTmab-PPLNs (0.34 ± 0.09) was about 0.03 times, 0.18 times, and 0.37 times those of DTX solution (10.50 ± 1.25), PPLNs (1.89 ± 0.26), pTmab-PPLNs (0.91 ± 0.15), respectively. For MCF7 cells, although the IC₅₀ value of eTmab-PPLNs (0.36 ± 0.02) was about 0.14 times that of DTX solution (2.59 ± 0.85), there was almost no difference between the IC₅₀ values of PPLNs (0.39 ± 0.05), pTmab-PPLNs (0.38 ± 0.04), and eTmab-PPLNs (0.36 ± 0.02).

Cellular Uptake by Confocal Microscopy

We used CLSM to visually observe drug distribution in BT474 and MCF7 cells after internalization of PPLNs or eTmab-PPLNs. Figure 8 shows the uptake of eTmab-PPLNs and PPLNs by BT474 and MCF7 cells, respectively. Among them, blue fluorescence represented the nuclei labeled by DAPI, green fluorescence represented FITC-labeled Tmab shell, red fluorescence represented the hydrophobic rhodamine B-loaded PPLNs core, and merged image represented the superposition of the above 3 images. For BT474 cells treated with double fluorescently labeled eTmab-PPLNs, it could be seen from the merged image that red fluorescence and green fluorescence overlapped, and the nuclei were surrounded by yellow

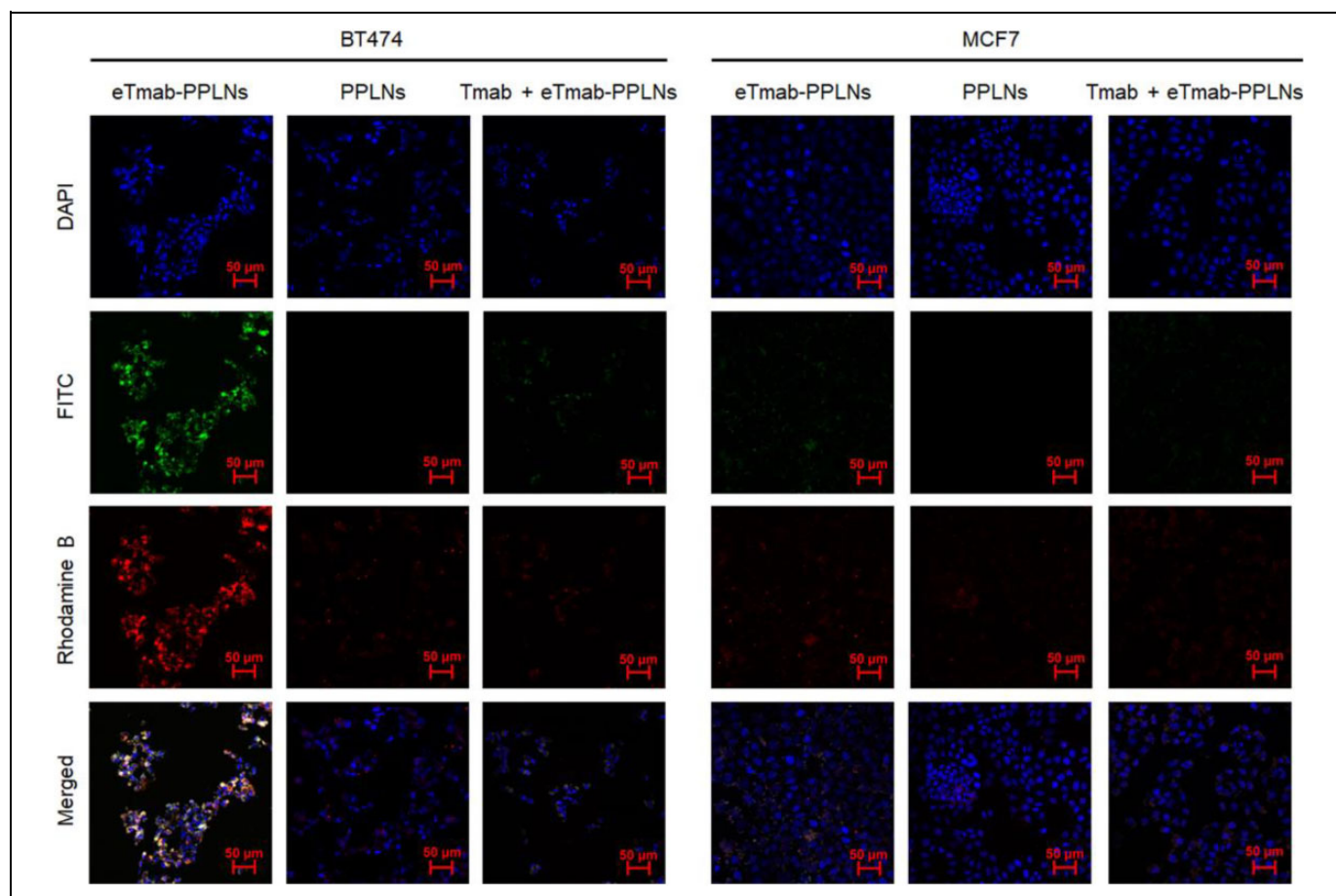


Figure 8. CLSM images of BT474 and MCF7 cells. BT474 and MCF7 cells were incubated with fluorescence-labeled PPLNs, eTmab-PPLNs, or Tmab + eTmab-PPLNs. Among them, Tmab + eTmab-PPLNs were represented free nonfluorescent labeled Tmab was added prior to the addition of double fluorescence labeled eTmab-PPLNs. CLSM indicates confocal laser scanning microscopy; eTmab-PPLNs, electrostatically conjugated trastuzumab-bearing poly (D, L-lactide-co-glycolide)/polyethylenimine/lipid nanoparticles; PPLNs, poly (D, L-lactide-co-glycolide)/polyethylenimine/lipid nanoparticles; Tmab, trastuzumab.

fluorescence (superimposed fluorescence), which proved that PPLNs and Tmab entered the cells at the same time, and Tmab did not dissociate from PPLNs during endocytosis.

As shown in Figure 8, the fluorescence intensity of eTmab-PPLNs in BT474 cells was significantly stronger than that of PPLNs. In contrast, there was no significant difference in uptake of the 2 formulations in MCF7 cells. These results indicated that the uptake of eTmab-PPLNs by BT474 cells was enhanced by HER2-mediated endocytosis. In addition, compared to the fluorescence intensity of eTmab-PPLNs in BT474 cells, the fluorescence intensity of Tmab + eTmab-PPLNs (free unlabeled Tmab was added prior to the addition of double fluorescence-labeled eTmab-PPLNs for blocking HER2) was significantly weaker. This result further demonstrated that eTmab-PPLNs could enhance HER2-positive cells uptake of Tmab through HER2-mediated endocytosis.

Cellular Uptake by Flow Cytometry

In order to observe the internalization of nanoparticles by BT474 and MCF7 cells, we also performed flow cytometry

experiments. As shown in Figure 9, the abscissa and ordinate indicated the fluorescence intensity of FITC and rhodamine B, respectively. The percentage of BT474 cells that internalized double fluorescence-labeled eTmab-PPLNs was significantly greater than that of MCF7 cells, and the ability of BT474 cells treated with Tmab + eTmab-PPLNs to uptake double fluorescence-labeled eTmab-PPLNs was diminished. This further illustrated the receptor targeting effect of Tmab.

Discussion

Antibodies against specific receptors on tumor cells attached to the nanoparticles surface can deliver drugs efficiently and specifically.^{41,42} Human epidermal growth factor receptor 2 is overexpressed in breast cancer.³¹⁻³³ Therefore, Tmab was used to enhance the targeting of nanoparticles for delivery of DTX. Here, the emulsifying solvent volatilization method was used to prepare nanoparticles, which produced nanoparticles with small particle sizes.^{43,44} Docetaxel was carried out using PLGA, egg PC, and PEI as substrates. Among them, egg PC was used to improve the biocompatibility of nanoparticles, and

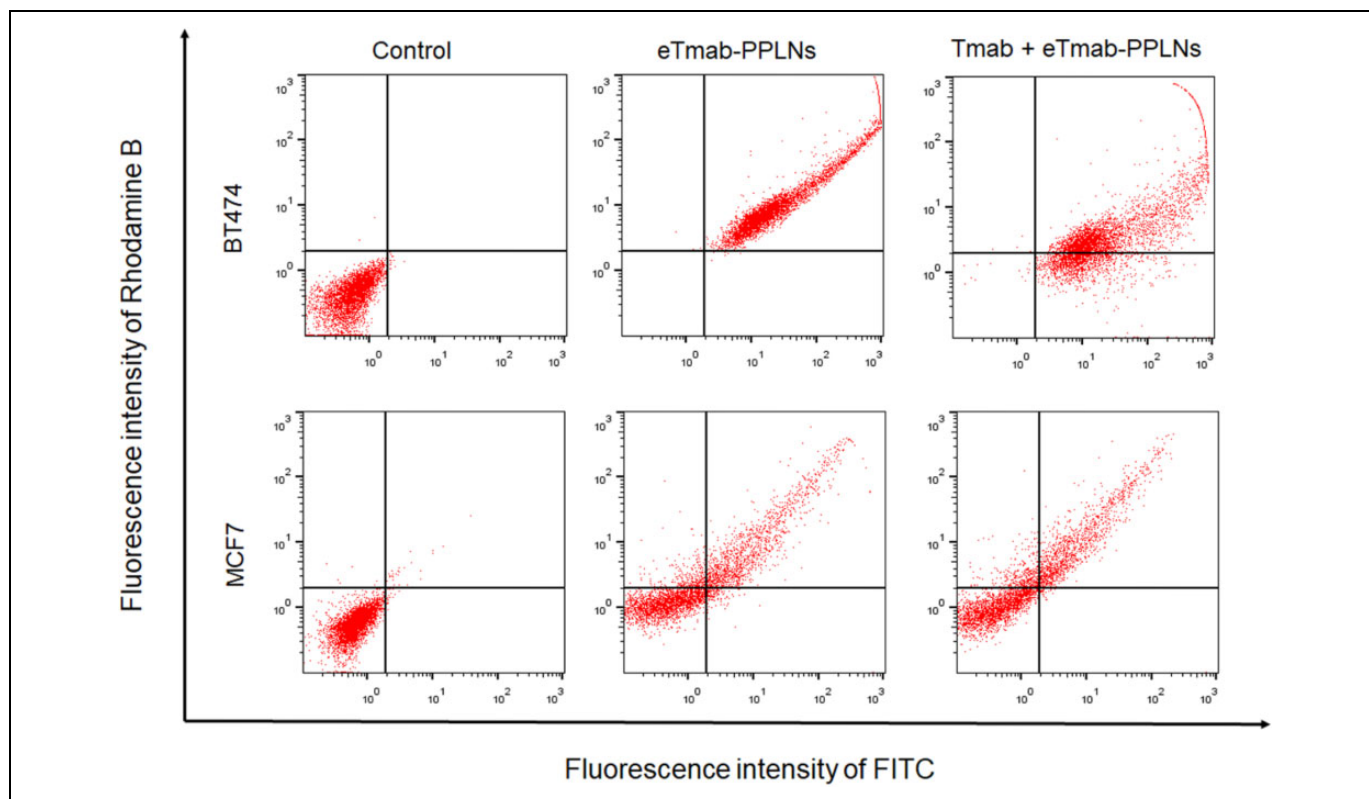


Figure 9. Cellular uptake efficiency of BT474 and MCF7 cells determined by flow cytometry. BT474 and MCF7 cells were treated with medium, double fluorescence labeled eTmab-PPLNs or Tmab + eTmab-PPLNs. Tmab + eTmab-PPLNs represented free Tmab preincubation plus fluorescence labeled eTmab-PPLNs. eTmab-PPLNs indicates electrostatically conjugated trastuzumab-bearing poly (D, L-lactide-co-glycolide)/polyethylenimine/lipid nanoparticles; PPLNs, poly (D, L-lactide-co-glycolide)/polyethylenimine/lipid nanoparticles; Tmab, trastuzumab.

PEI as a cationic polymer was used to provide positive charge on the surface of PPLNs to facilitate electrostatic adsorption with Tmab.

After the addition of Tmab, the increase in particle size of nanoparticles may be because of the effective attachment of Tmab to the surface of nanoparticles. In addition, because of the presence of PEI in nanoparticles, the surface ζ potential was positive, while the ζ potential was decreased after adsorption of Tmab, which indicated that the Tmab adsorbed on the surface of PPLNs neutralized the ζ potential of PPLNs.⁴⁰ Binding efficiency is defined as the percentage of the amount of adsorbed Tmab and the total amount of Tmab added in the preparation process. This involves the problem of utilization of expensive antibody. Enhancing antibody binding rate and reducing the amount of antibody can reduce the cost of nanoparticles preparation. When PPLNs-Tmab was at a low ratio, a large number of free Tmab in the system would cause waste of Tmab.

The particle size of eTmab-PPLNs measured by DLS (217.4 nm) was bigger than that measured by TEM (about 130 nm). This difference might be due to that in DLS the size was measured in aqueous solution, while TEM measured was performed on dehydrated nanoparticles.⁴⁵ The particle size measured by DLS was not the actual size of nanoparticles, but the hydrated particle size. When the nanoparticles were dispersed in solution, there would be a layer of hydration layer

on the surface. The particle size measured by DLS includes the hydration layer, so the particle size would be larger. TEM measures dry samples without a hydrated layer, so the particle size was relatively small.

In the nanoparticle stability test, the PDI of eTmab-PPLNs was less than 0.3 at 37°C and 4°C, indicating that the dispersibility and stability were good, which is important for the storage, transportation, and use of nanoparticles. As shown in Figure 5, the PPLNs and eTmab-PPLNs were in a biphasic release mode: initial burst release was observed followed by sustained release characteristic. During a period of time at the beginning, the PPLNs and eTmab-PPLNs surface drug were quickly released by diffusion. Then, the drug-coated polymer was eroded, which resulted in further drug release. In vitro release results indicated that DTX released from PPLNs and eTmab-PPLNs was relatively rapid, which was helpful to reach the therapeutic window and was beneficial to the treatment of tumor.

The inhibitory effects of DTX-loaded eTmab-PPLNs and their components (DTX, Tmab, PPLNs, eTmab-PPLNs, and pTmab-PPLNs) on BT474 and MCF7 cells proliferation were investigated. Compared with BT474 and MCF7 cells, eTmab-PPLNs were found to be more cytotoxic to BT474 cells. Compared with PPLNs, pTmab-PPLNs, and eTmab-PPLNs, eTmab-PPLNs showed the strongest cytotoxicity to BT474

cells. These indicated that the electrostatic adsorption of Tmab on nanoparticles could be recognized by HER2 on HER2-positive cells, and the DTX-loaded nanoparticles could better act on cancer cells. These also indicated that the electrostatic adsorption method was less harmful to the Tmab antigen recognition region.

Two experiments commonly used to observe the uptake of nanoparticles in cells were performed: laser confocal and flow cytometry experiments. In the laser confocal experiment, there was a number of yellow areas around the nucleus of BT474 cells incubated by eTmab-PPLNs, indicating that Tmab and PPLNs were internalized at the same time, and the electrostatic adsorption between Tmab and PPLNs was relatively stable. In order to verify the targeting efficiency of Tmab, BT474 cells were treated with excess free Tmab to block HER2 before drug administration. The results showed that the uptake ability of BT474 cells treated with Tmab + eTmab-PPLNs was greatly reduced. Meanwhile, the flow cytometry experiment showed the same trend as shown in Figure 9. These results also supported the results of cytotoxicity: Tmab could target HER2-positive breast cancer cell as a targeting ligand to promote uptake of eTmab-PPLNs by cancer cells.

Conclusions

In this study, targeted nanoparticles were prepared by combining PPLNs with Tmab through electrostatic adsorption method to deliver antitumor drug DTX. Through screening a series of formulations, eTmab-PPLNs with small particle size, smooth and round shape, good biocompatibility, and great stability were prepared. The results of cellular uptake and in vitro cytotoxicity experiments also showed that eTmab-PPLNs could efficiently transport DTX to HER2-positive breast cancer cells, which had a cell-targeting effect and could effectively inhibit the proliferation of cancer cells. This work demonstrates that eTmab-PPLNs are promising to treat breast cancer with high HER2 expression.


Declaration of Conflicting Interests


The author(s) declared no potential conflicts of interest with respect to the research, authorship, and/or publication of this article.

Funding

The author(s) disclosed receipt of the following financial support for the research, authorship, and/or publication of this article: This research was supported by Jilin Province Science and Technology Development Program (No. 20180101269JC) and the State Key Laboratory of Long-Acting and Targeting Drug Delivery System and Shandong Luye Pharmaceutical Co, Ltd.

ORCID iD

Fengying Sun  <https://orcid.org/0000-0001-6199-9311>

Lesheng Teng  <https://orcid.org/0000-0003-1623-5384>

References

1. Siegel RL, Miller KD, Jemal A. Cancer statistics, 2018. *CA Cancer J Clin.* 2018;68(1):7-30.
2. Chen W, Zheng R, Baade PD, et al. Cancer statistics in China, 2015. *CA Cancer J Clin.* 2016;66(2):115-132.
3. Torre LA, Bray F, Siegel RL, Ferlay J, Lortet-Tieulent J, Jemal A. Global cancer statistics, 2012. *CA Cancer J Clin.* 2015;65(2):87-108.
4. Ferlay J, Soerjomataram I, Dikshit R, et al. Cancer incidence and mortality worldwide: sources, methods and major patterns in GLOBOCAN 2012. *Int J Cancer.* 2015;136(5):E359-E386.
5. Mazzaferro S, Bouchemal K, Ponchel G. Oral delivery of anticancer drugs I: general considerations. *Drug Discov Today.* 2013;18(1-2):25-34.
6. Veronesi U, Boyle P, Goldhirsch A, Orecchia R, Viale G. Breast cancer. *Lancet.* 2005;365(9472):1727-1741.
7. Clarke SJ, Rivory LP. Clinical pharmacokinetics of docetaxel. *Clin Pharmacokinet.* 1999;36(2):99-114.
8. Bissery MC. Preclinical pharmacology of docetaxel. *Eur J Cancer.* 1995;31A(Suppl 4):S1-S6.
9. Ringel I, Horwitz SB. Studies with RP 56976 (taxotere): a semi-synthetic analogue of taxol. *J Natl Cancer Inst.* 1991;83(4):288-291.
10. Schrijvers D, Wanders J, Dirix L, et al. Coping with toxicities of docetaxel (Taxotere). *Ann Oncol.* 1993;4(7):610-611.
11. Wang HX, Lu ZJ, Wang LJ, et al. New generation nanomedicines constructed from self-assembling small-molecule prodrugs alleviate cancer drug toxicity. *Cancer Res.* 2017;77(24):6963-6974.
12. Wan JQ, Qiao YT, Chen XN, et al. Structure-guided engineering of cytotoxic cabazitaxel for an adaptive nanoparticle formulation: enhancing the drug safety and therapeutic efficacy. *Adv Funct Mater.* 2018;28(52):1804229.
13. Wang HX, Wu JP, Xu L, Xie K, Chen C, Dong YH. Albumin nanoparticle encapsulation of potent cytotoxic therapeutics shows sustained drug release and alleviates cancer drug toxicity. *Chem Commun.* 2017;53(17):2618-2621.
14. Fang T, Ye ZJ, Wu JP, Wang HX. Reprogramming axial ligands facilitates the self-assembly of a platinum(IV) prodrug: overcoming drug resistance and safer in vivo delivery of cisplatin. *Chem Commun.* 2018;54(66):9167-9170.
15. Wang HX, Zhou LQ, Xie K, et al. Polylactide-tethered prodrugs in polymeric nanoparticles as reliable nanomedicines for the efficient eradication of patient-derived hepatocellular carcinoma. *Theranostics.* 2018;8(14):3949-3963.
16. Wang HX, Chen JM, Xu C, et al. Cancer nanomedicines stabilized by pi-pi stacking between heterodimeric prodrugs enable exceptionally high drug loading capacity and safer delivery of drug combinations. *Theranostics.* 2017;7(15):3638-3652.
17. Garg NK, Singh B, Sharma G, et al. Development and characterization of single step self-assembled lipid polymer hybrid nanoparticles for effective delivery of methotrexate. *RSC Advances.* 2015;5(77):62989-62999.
18. Mandal B, Bhattacharjee H, Mittal N, et al. Core-shell-type lipid-polymer hybrid nanoparticles as a drug delivery platform. *Nano-medicine.* 2013;9(4):474-491.
19. Zhang L, Chan JM, Gu FX, et al. Self-assembled lipid-polymer hybrid nanoparticles: a robust drug delivery platform. *ACS Nano.* 2008;2(8):1696-1702.

20. Hadinoto K, Sundaresan A, Cheow WS. Lipid-polymer hybrid nanoparticles as a new generation therapeutic delivery platform: a review. *Eur J Pharm Biopharm.* 2013;85(3 Pt A):427-443.
21. Das M, Mohanty C, Sahoo SK. Ligand-based targeted therapy for cancer tissue. *Expert Opin Drug Deliv.* 2009;6(3):285-304.
22. Vasir JK, Labhasetwar V. Targeted drug delivery in cancer therapy. *Technol Cancer Res Treat.* 2005;4(4):363-374.
23. Bethge WA, Sandmaier BM. Targeted cancer therapy and immunosuppression using radiolabeled monoclonal antibodies. *Semin Oncology.* 2004;31(1):68-82.
24. Rao AV, Schmader K. Monoclonal antibodies as targeted therapy in hematologic malignancies in older adults. *Am J Geriatr Pharmacother.* 2007;5(3):247-262.
25. Fischer OM, Streit S, Hart S, Ullrich A. Beyond herceptin and gleevec. *Curr Opin Chem Biol.* 2003;7(4):490-495.
26. Piccart-Gebhart MJ, Procter M, Leyland-Jones B, et al. Trastuzumab after adjuvant chemotherapy in HER2-positive breast cancer. *N Engl J Med.* 2005;353(16):1659-1672.
27. Romond EH, Perez EA, Bryant J, et al. Trastuzumab plus adjuvant chemotherapy for operable HER2-positive breast cancer. *N Engl J Med.* 2005;353(16):1673-1684.
28. Vogel CL, Cobleigh MA, Tripathy D, et al. Efficacy and safety of trastuzumab as a single agent in first-line treatment of HER2-overexpressing metastatic breast cancer. *J Clin Oncol.* 2002; 20(3):719-726.
29. Slamon DJ, Godolphin W, Jones LA, et al. Studies of the HER-2/neu proto-oncogene in human breast and ovarian cancer. *Science.* 1989;244(4905):707-712.
30. Slamon DJ, Clark GM, Wong SG, Levin WJ, Ullrich A, McGuire WL. Human breast cancer: correlation of relapse and survival with amplification of the HER-2/neu oncogene. *Science.* 1987; 235(4785):177-182.
31. Wiseman SM, Makretsov N, Nielsen TO, et al. Coexpression of the type 1 growth factor receptor family members HER-1, HER-2, and HER-3 has a synergistic negative prognostic effect on breast carcinoma survival. *Cancer.* 2005;103(9):1770-1777.
32. Nguyen KCT, Muthiah M, Islam MA, et al. Selective transfection with osmotically active sorbitol modified PEI nanoparticles for enhanced anti-cancer gene therapy. *Colloids Surf B Biointerfaces.* 2014;119:126-136.
33. Nimesh S, Chandra R. Polyethylenimine nanoparticles as an efficient in vitro siRNA delivery system. *Eur J Pharm Biopharm.* 2009;73(1):43-49.
34. Yu KT, Zhao JL, Zhang ZK, et al. Enhanced delivery of paclitaxel using electrostatically-conjugated herceptin-bearing PEI/PLGA nanoparticles against HER-positive breast cancer cells. *Int J Pharm.* 2016;497(1-2):78-87.
35. Pitts MS, McShane JN, Hoener MC, Christian SL, Berry MD. TAAR1 levels and sub-cellular distribution are cell line but not breast cancer subtype specific. *Histochem Cell Biol.* 2019;152(2): 155-166.
36. Chan JM, Zhang LF, Yuet KP, et al. PLGA-lecithin-PEG core-shell nanoparticles for controlled drug delivery. *Biomaterials.* 2009;30(8):1627-1634.
37. Kumar M, Bakowsky U, Lehr CM. Preparation and characterization of cationic PLGA nanospheres as DNA carriers. *Biomaterials.* 2004;25(10):1771-1777.
38. Lee ALZ, Wang Y, Cheng HY, Pervaiz S, Yang YY. The co-delivery of paclitaxel and Herceptin using cationic micellar nanoparticles. *Biomaterials.* 2009;30(5):919-927.
39. Yang MD, Ding JX, Zhang Y, et al. Activated macrophage-targeted dextran-methotrexate/folate conjugate prevents deterioration of collagen-induced arthritis in mice. *J Mat Chem B.* 2016;4(12):2102-2113.
40. Acharya S, Dilnawaz F, Sahoo SK. Targeted epidermal growth factor receptor nanoparticle bioconjugates for breast cancer therapy. *Biomaterials.* 2009;30(29):5737-5750.
41. Prabhu RH, Patravale VB, Joshi MD. Polymeric nanoparticles for targeted treatment in oncology: current insights. *Int J Nanomed.* 2015;10:1001-1018.
42. Shargh VH, Hondermarck H, Liang MT. Antibody-targeted biodegradable nanoparticles for cancer therapy. *Nanomedicine.* 2016;11(1):63-79.
43. Anton N, Benoit JP, Saulnier P. Design and production of nanoparticles formulated from nano-emulsion templates—a review. *J Control Release.* 2008;128(3):185-199.
44. Staff RH, Landfester K, Crespy D. Recent advances in the emulsion solvent evaporation technique for the preparation of nanoparticles and nanocapsules. In: Percec V, ed. *Hierarchical Macromolecular Structures: 60 Years after the Staudinger Nobel Prize II.* Vol 262. Cham, Switzerland: Springer International Publishing Ag; 2013:329-344.
45. Abouelmagd SA, Meng FF, Kim BK, Hyun H, Yeo Y. Tannic acid-mediated surface functionalization of polymeric nanoparticles. *ACS Biomater Sci Eng.* 2016;2(12):2294-2303.